



Drift Stabilisation of Ballooning Modes in a High- $\langle\beta\rangle$ LHD Configuration

W. A. Cooper¹, L. Brocher¹, J. P. Graves¹, G. A. Cooper²,
Y. Narushima³ and K. Y. Watanabe³

¹Ecole Polytechnique Fédérale de Lausanne (EPFL), Association EURATOM-Confédération Suisse, Centre de
Recherches en Physique des Plasmas, CH1015 Lausanne, Switzerland.

²University of the South, Sewanee, TN 37383, USA.

³National Institute for Fusion Science, Oroschi-cho 322-6, Toki 509-5292, Japan



Motivation and Background (1)

- The high- β LHD discharges $\langle \beta_{dia} \rangle \sim 5\%$ are obtained with an inward shifted configuration, low density ($< 3 \times 10^{-19} m^{-3}$), strong tangential neutral beam injection ($\sim 14 MW; \sim 150 - 180 keV$) (Weller et al., Nucl. Fusion 49 (2009) 065016-1-13).
- At low densities, the pressure anisotropy driven by the neutral beam ions can be very significant (T. Yamaguchi et al., Nucl. Fusion 45 (2005) L33).
- Ideal MHD as well as other anisotropic pressure single fluid models (Kruskal-Oberman; Johnson-Kulsrud-Weimer) predict ballooning instability in Heliotron devices well below the experimentally achieved $\langle \beta \rangle$ values in LHD.
- The LHD experimental data points align with the theoretically calculated ideal MHD stability diagrams for global $n = 1$ modes when the hot particle contributions to the pressure gradients are neglected (K. Y. Watanabe et al., Nucl. Fusion 45 (2005) 1247).



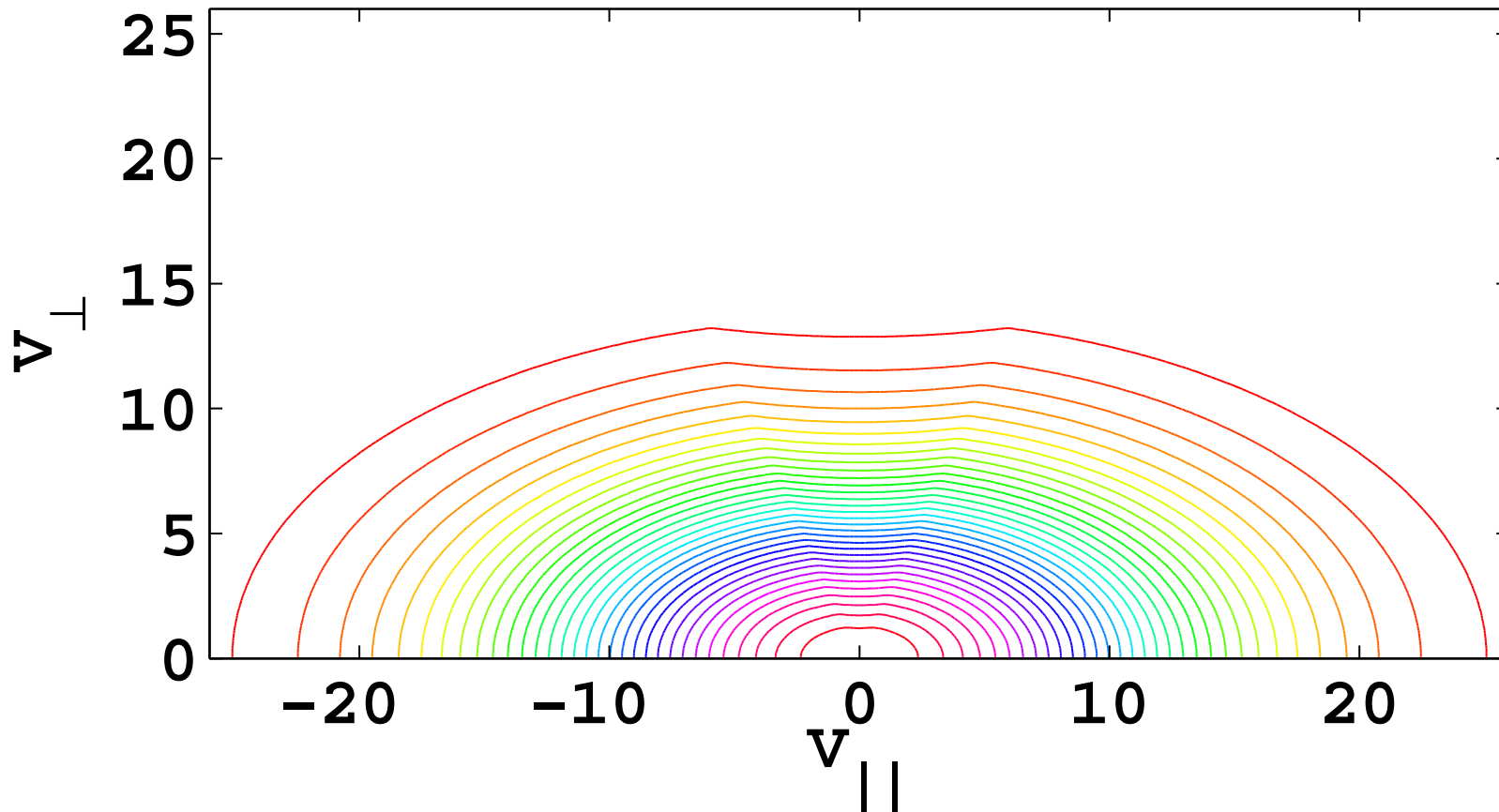
Motivation and Background (2)

- The ballooning criteria are particularly severe for field lines that cross the regions with most destabilising magnetic field line curvature.
- Finite radial corrections require the evaluation of ballooning stability on all field lines and all radial wave numbers. For pressure profiles that are more peaked than in the experiment, the unstable domains are topologically spherical (Nakajima et al., FST 51 (2007) 79) and global structures are difficult to construct leading to inconclusive stability predictions. For profiles that are box-like (broader than in the experiment), the ballooning unstable domains are topologically cylindrical from which unstable global structures can be computed (Cooper-Singleton-Dewar , Phys. Plasmas 3 (1996) 275, 3520(E)).
- We explore whether a drift-magnetohydrodynamic model can more adequately describe the stability properties observed in LHD at high $\langle \beta_{dia} \rangle$.

- Apply the ANIMEC code (Cooper et al., Comput. Phys. Commun. (2009) in press) for the computation of anisotropic pressure equilibria to model the inward-shifted LHD configuration at high- $\langle\beta\rangle$.
- A drift-magnetohydrodynamic (MHD) ballooning mode equation derived from the linearised gyrokinetic equation is applied to investigate the local stability properties.
- Eigenvalues in the single fluid limit are computed using the BECOOL ballooning stability solver (G. A. Cooper et al., J. Comput. Phys. 228 (2009) 4911). A perturbative approach yields a quadratic dispersion relation for the mode frequency and the growth rate in the drift-MHD model.
- The validity of the approximations leading to the drift-MHD ballooning equation applied are verified.
- Summary and Conclusions.

The MHD Equilibrium State

- 3D anisotropic pressure equilibria that model the LHD inward-shifted configuration are computed with the ANIMEC code.
- The hot particle pressures are calculated from the moments of a bi-Maxwellian distribution function.





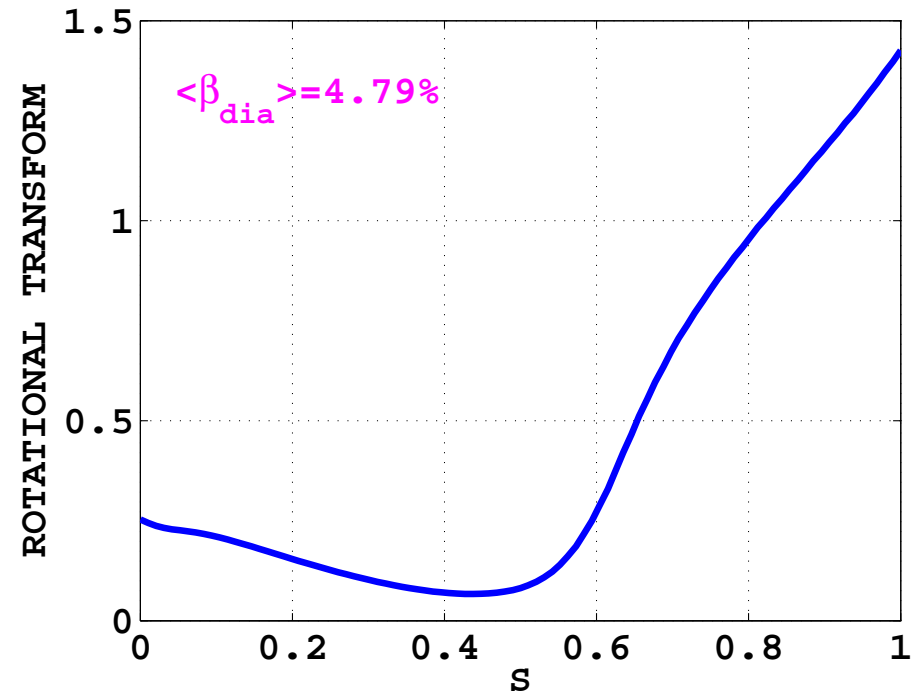
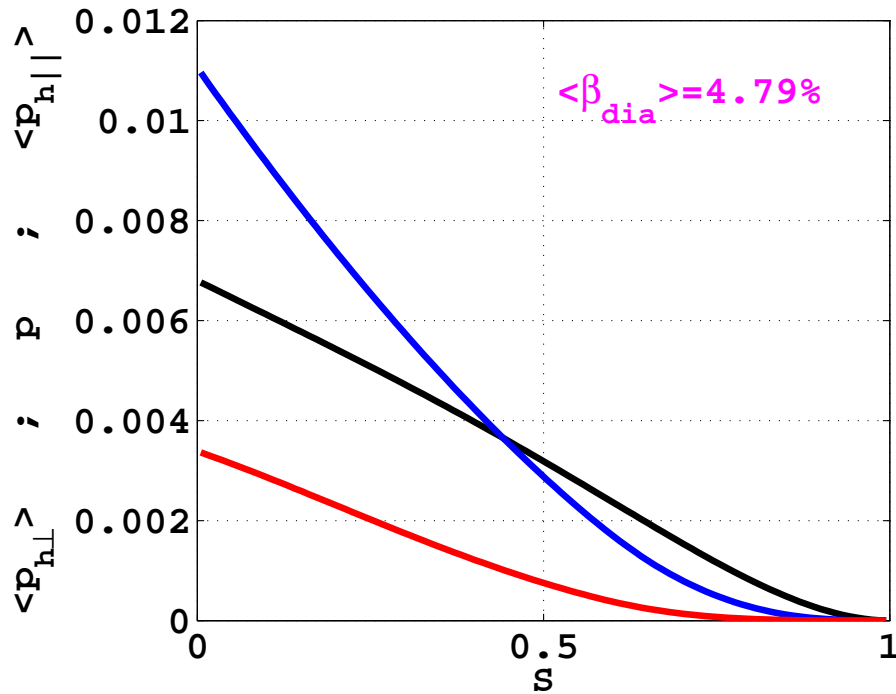
Input Profiles and Parameters for 3D Equilibria

- The hot particle deposition layer is concentrated around a magnetic field value $B_C = 0.425T$. The profiles required for the equilibrium calculation are:
 - Thermal pressure: $p(s) = p(0)(1 - s)(1 - s^4)$.
 - Hot particle pressure amplitude: $p_h(s) = p_{\mathcal{H}}(1 - s)$.
 - Anisotropy factor: $[T_{\perp}/T_{\parallel}](s) = [T_{\perp}/T_{\parallel}](0)(1 - s^2)$.
 - Toroidal current: $2\pi J(s) = 0$.
 - Radial variable: $0 \leq s \leq 1$ (\propto enclosed toroidal magnetic flux).
 - $p(0)$ and $p_{\mathcal{H}}$ are chosen so that $\langle \beta_{dia} \rangle = \langle 2\mu_0 p_{\perp} / B^2 \rangle \simeq 4.79\%$ and $\langle \beta_{th} \rangle = \langle 2\mu_0 p / B^2 \rangle \simeq 3.53\%$.
 - $[T_{\perp}/T_{\parallel}](0) = 1/3$ yields $\langle \beta_{\parallel} \rangle / \langle \beta_{dia} \rangle \simeq 1.62$.
- Maximum experimentally achieved $\langle \beta_{dia} \rangle \simeq 4.8\%$ (Weller et al., Nucl. Fusion 49 (2009) 065016-1-13).



Pressure and Rotational Transform Profiles

- Pressure profiles
- Rotational transform profile at $\langle \beta_{dia} \rangle = 4.79\%$



Drift-MHD Ballooning Stability Equation

- The TERPSICHORE code is used to transform the equilibrium state computed with ANIMEC to Boozer magnetic coordinates (Cooper, PPCF 34 (1992) 1011).
- Starting point: Linearised gyrokinetic equation in ballooning space (Catto-Tang-Baldwin, Plasma Phys. 23 (1981) 69).
- Critical assumption for drift-corrected MHD model: $\omega/\omega_{dh} \ll 1$.
- Resulting ballooning equation in variational form (Cooper, Phys. Fluids 26 (1983) 1834)

$$\begin{aligned}
 & \int_{-\infty}^{\infty} d\theta \left\{ \frac{\sigma k_{\perp}^2}{\sqrt{g} B^2} |\sqrt{g} \mathbf{B} \cdot \nabla \chi|^2 \right. \\
 & - \left. \frac{k_{\alpha} \sqrt{g} p'(s)}{\psi'(s) B^2} \left[\left(1 + \frac{\sigma}{\tau} \right) \mathbf{B} \times \mathbf{k}_{\perp} \cdot \boldsymbol{\kappa} - \frac{k_{\alpha}}{\psi'(s)} \frac{\partial p_{\perp h}}{\partial s} \Big|_B \right] |\chi|^2 \right\} \\
 & = \int_{-\infty}^{\infty} d\theta M_i N_i \frac{\sqrt{g} k_{\perp}^2}{B^2} \omega \left[\omega - \left(\omega_{*pi} + \frac{M_h N_h \omega_{*h}}{M_i N_i b_h} \right) \right] |\chi|^2
 \end{aligned}$$

Ballooning Equation Parameters

- Magnetic field: B
- Curvature: $\kappa = (b \cdot \nabla)b$
- Jacobian: \sqrt{g}
- Poloidal flux: $2\pi\psi$
- Particle mass, density: M_ℓ, N_ℓ ($i = \text{ion}, h = \text{hot particle}$)
- Wave vector: $k_\perp = k_\alpha[\nabla\phi - q(s)\nabla\theta - q'(s)(\theta - \theta_k)\nabla s]$
- Firehose stability parameter: $\sigma = \frac{1}{\mu_0} - \frac{1}{B} \frac{\partial p_\parallel}{\partial B} \Big|_s$
- Mirror stability parameter: $\tau = \frac{1}{\mu_0} + \frac{1}{B} \frac{\partial p_\perp}{\partial B} \Big|_s$
- Thermal ion diamagnetic drift frequency: $\omega_{*pi} = -\frac{k_\alpha p'(s)}{2Z_i e \psi'(s) N_i}$
- Hot ion diamagnetic drift frequency: $\omega_{*h} = -\frac{k_\alpha p_{\perp h}}{Z_h e \psi'(s) N_h^2} \frac{\partial N_h}{\partial s} \Big|_B$
- Hot particle Larmor radius term: $b_h = k_\perp^2 \rho_h^2 = \frac{k_\perp^2 p_{\perp h} M_h}{Z_h^2 e^2 B^2 N_h}$
- Unit vector along B : $b = B/|B|$
- Inverse rotational transform: q
- Boozer angles: θ, ϕ
- Radial wave number: $\theta_k \equiv k_q/k_\alpha$

- Hot particle density: $N_h(s, B) = N_h(s, B_C)\mathcal{C}(s, B)$

- For $B \geq B_C$

$$\mathcal{C}(s, B) = \frac{\frac{B}{B_C}}{1 - \frac{T_{\perp}}{T_{\parallel}} \left(1 - \frac{B}{B_C}\right)}$$

- For $B < B_C$

$$\mathcal{C}(s, B) = \frac{\frac{B}{B_C}}{1 - \frac{T_{\perp}}{T_{\parallel}} \left(1 - \frac{B}{B_C}\right)} \left[1 - \frac{2 \left(\frac{T_{\perp}}{T_{\parallel}}\right)^{3/2} \left(1 - \frac{B}{B_C}\right)^{3/2}}{1 + \frac{T_{\perp}}{T_{\parallel}} \left(1 - \frac{B}{B_C}\right)} \right]$$

- Hot particle density profile chosen as: $N_h(s, B_C) = N_{h0}(1 - s)^2$



Observations About the Drift-Ballooning Equation

- The limit $\omega \ll \omega_{dh} \implies$ hot particles traverse unstable regions too quickly to significantly contribute to the instability drive. Consequently, the thermal ion and electron pressure gradients dominate the ballooning stability properties.
- Conversely, the term that involves the hot particle diamagnetic drift stabilisation ω_{*h} has a correction proportional to ρ_h^{-2} which shows that the larger the hot particle Larmor radius, the smaller the stabilisation effect.

- ▶ Obtained by imposing $\omega_{*pi} = \omega_{*h} = 0$
- ▶ Single fluid ballooning equation reduces to:

$$\begin{aligned}
 & \int_{-\infty}^{\infty} d\theta \left\{ \frac{\sigma k_{\perp}^2}{\sqrt{g} B^2} |\sqrt{g} \mathbf{B} \cdot \nabla \chi|^2 \right. \\
 & - \left. \frac{k_{\alpha} \sqrt{g} p'(s)}{\psi'(s) B^2} \left[\left(1 + \frac{\sigma}{\tau} \right) \mathbf{B} \times \mathbf{k}_{\perp} \cdot \boldsymbol{\kappa} - \frac{k_{\alpha}}{\psi'(s)} \frac{\partial p_{\perp h}}{\partial s} \Big|_B \right] |\chi|^2 \right\} \\
 & = -\gamma_F^2 \int_{-\infty}^{\infty} d\theta M_i N_i \frac{\sqrt{g} k_{\perp}^2}{B^2} |\chi|^2
 \end{aligned}$$

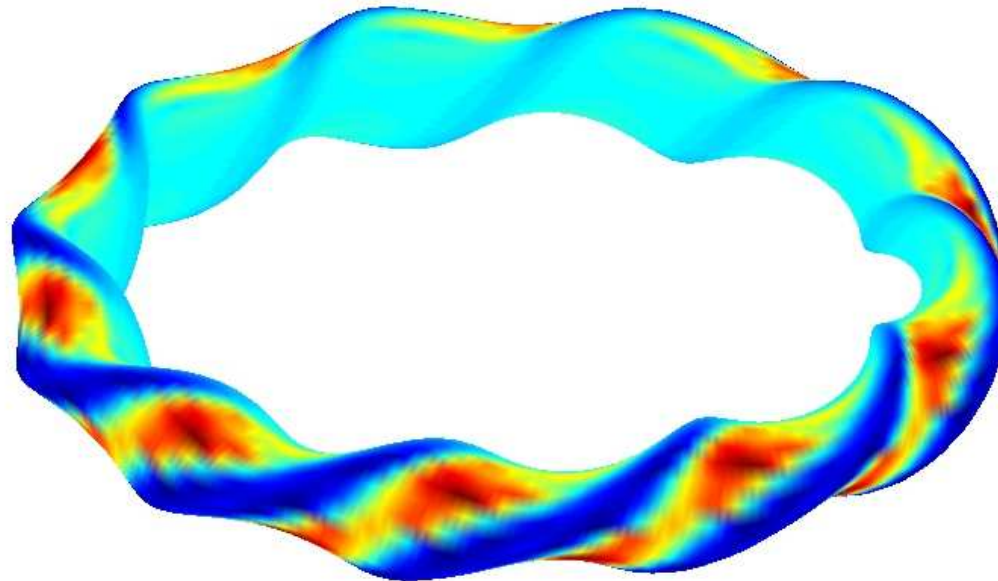
- ▶ $p_{\perp h} = 0 \implies \sigma/\tau = 1 \implies$ recovers incompressible ideal MHD

- ▶ Discretise χ using COOL finite elements based on variable-order Legendre polynomials. This reduces the variational problem to a special block-pentadiagonal matrix eigenvalue equation

$$AY = \lambda BY$$

- ▶ This is solved using an inverse vector iteration technique with the BECOOL code (G.A. Cooper et al., J. Comput. Phys. 228 (2009) 4911). The order of the polynomial chosen is typically cubic. The eigenvalue $\lambda \equiv -\gamma_F^2$.
- ▶ Concentrate on the field lines that traverse the most destabilising curvature region on each flux surface choosing the radial wave number $\theta_k = 0$.

- Flux surface corresponding to $s = 0.599$

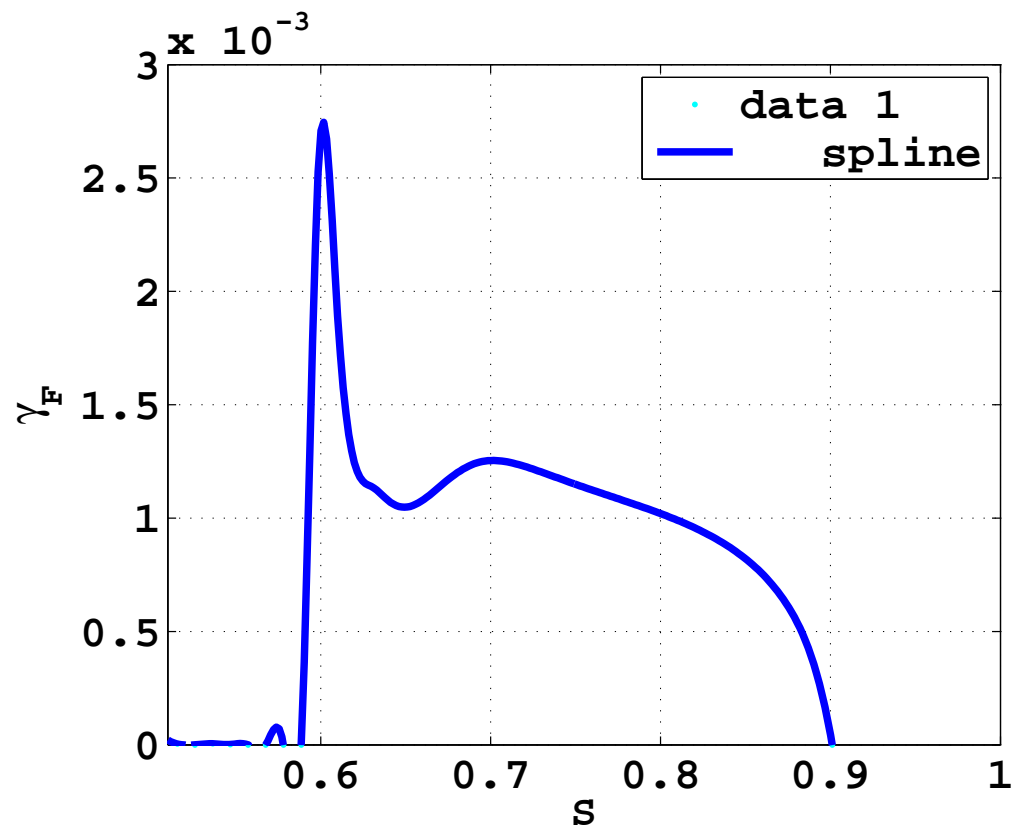
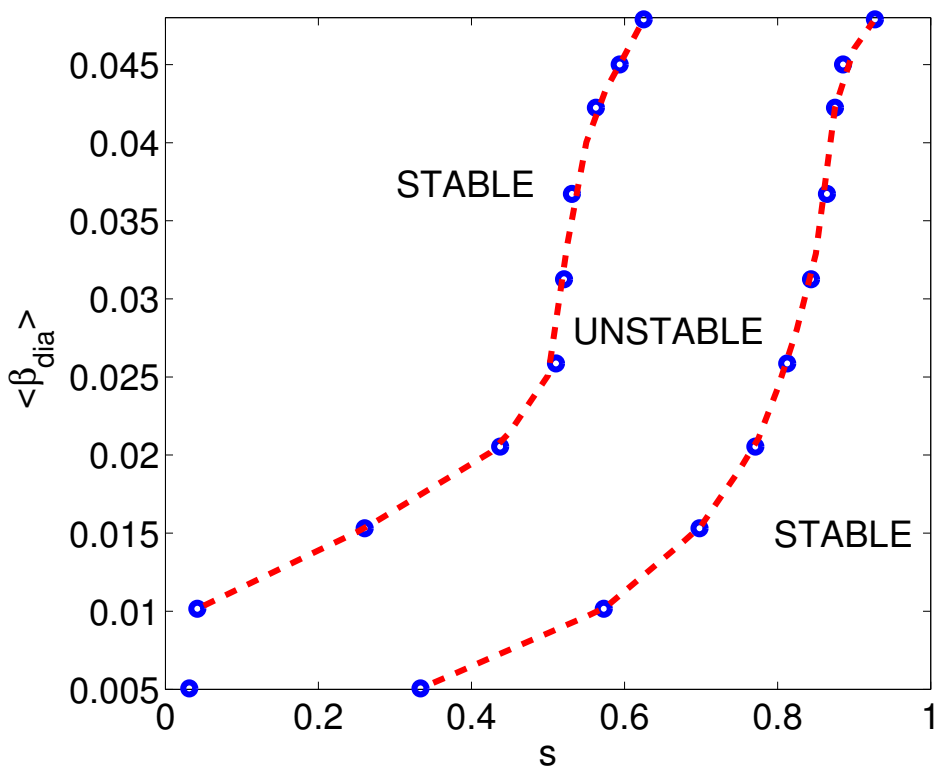




Single-Fluid Stability Diagram and Growth Rate

- Stability Diagram

- Fluid growth rate profile at $\langle \beta_{dia} \rangle \simeq 4.8\%$



- ▶ Apply perturbative approach using χ from the single-fluid ballooning model as a test eigenfunction.
- ▶ Derive the dispersion relation

$$\omega^2 - \omega(\omega_{*pi} + \omega_{*heff}) + \gamma_F^2 = 0$$

- ▶ The effective hot particle diamagnetic drift frequency is:

$$\begin{aligned} \omega_{*heff} &= \left\langle \frac{M_h N_h \omega_{*h}}{M_i N_i b_h} \right\rangle \\ &= \frac{\int_{-\infty}^{\infty} d\theta \frac{\sqrt{g}}{\psi'(s)} \left(\frac{k_{\perp}^2}{B^2} \right) \left(\frac{M_h N_h \omega_{*h}}{M_i N_i b_h} \right) |\chi|^2}{\int_{-\infty}^{\infty} d\theta \frac{\sqrt{g}}{\psi'(s)} \left(\frac{k_{\perp}^2}{B^2} \right) |\chi|^2} \end{aligned}$$



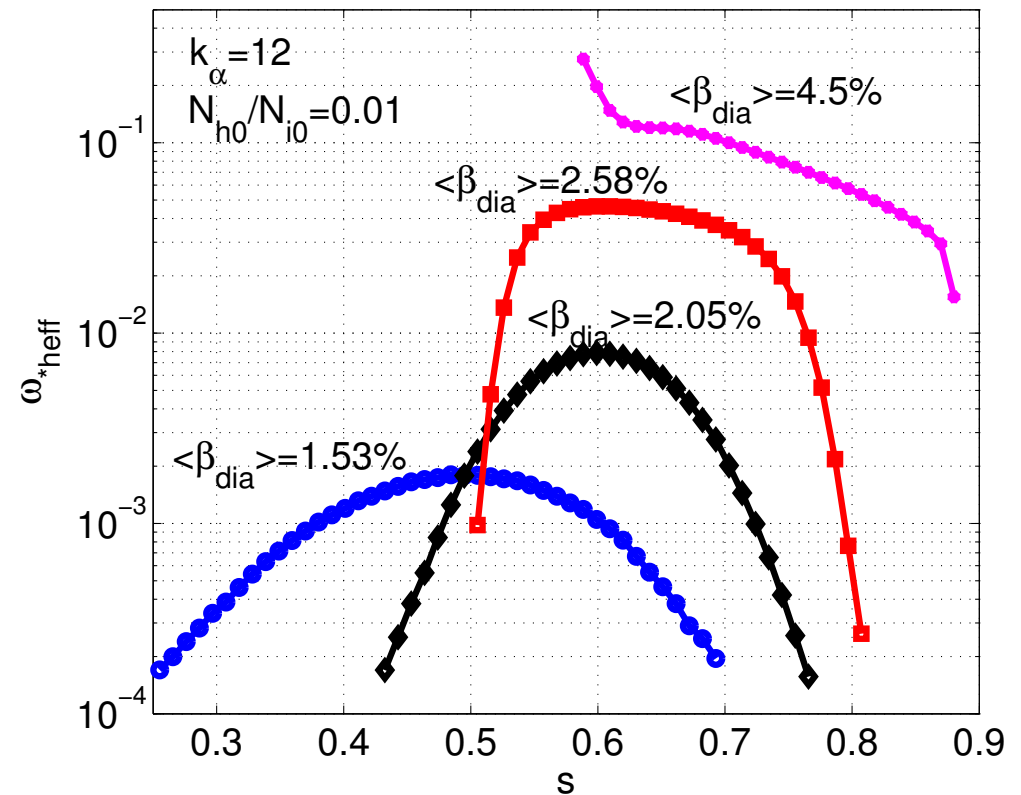
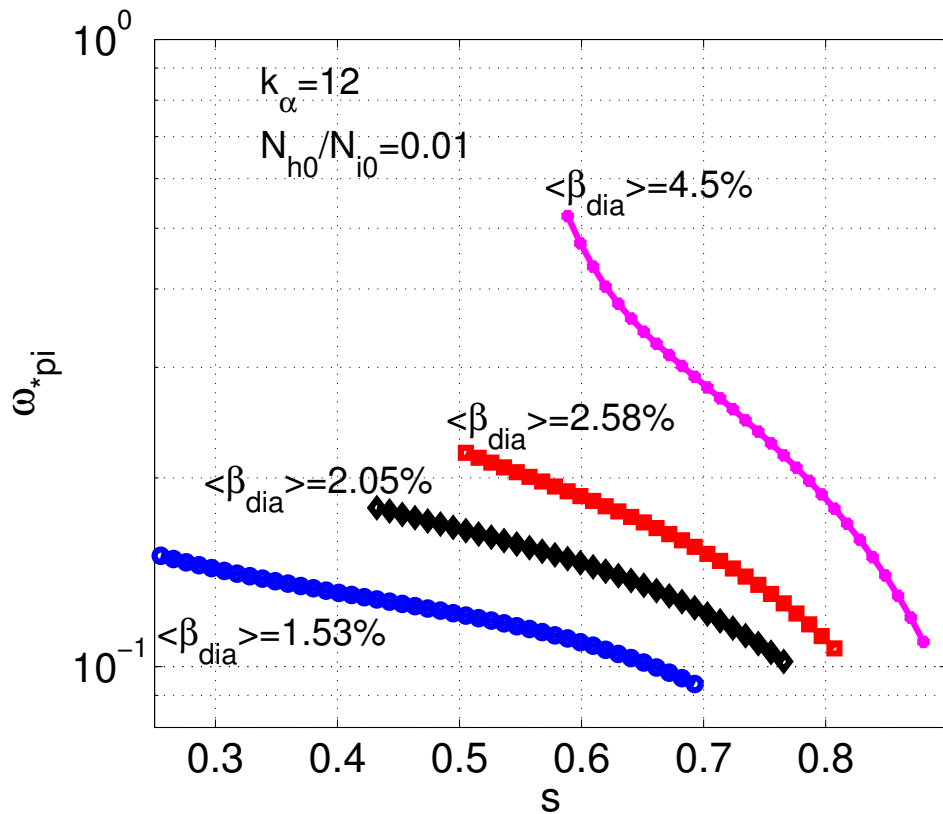
Ballooning study with diamagnetic drift corrections (2)

- ▶ The integrals in the numerator and the denominator are performed with the same Gauss-Legendre quadrature rule that is applied in the BECOOL code.
- ▶ All frequencies (and growth rates) are normalised to the toroidal Alfvén frequency $\omega_A = v_A/R_0$ where $v_A = B_0/\sqrt{(\mu_0 M_i N_{i0})}$.
- ▶ For $|\omega_{*pi} + \omega_{*heff}|/2 \geq \gamma_F$, the mode growth rate = 0. Complex frequency when $|\omega_{*pi} + \omega_{*heff}|/2 < \gamma_F$.
- ▶ In this study, we consider H -beam ions injected in a H -background plasma.

Diamagnetic Drift Frequency Profiles

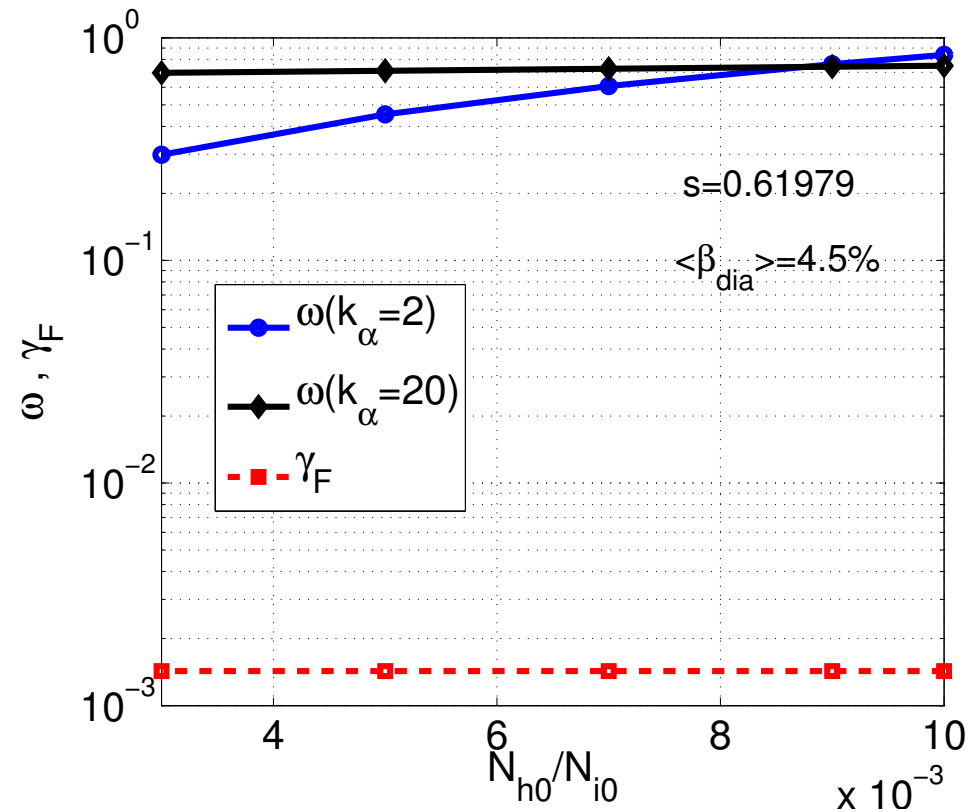
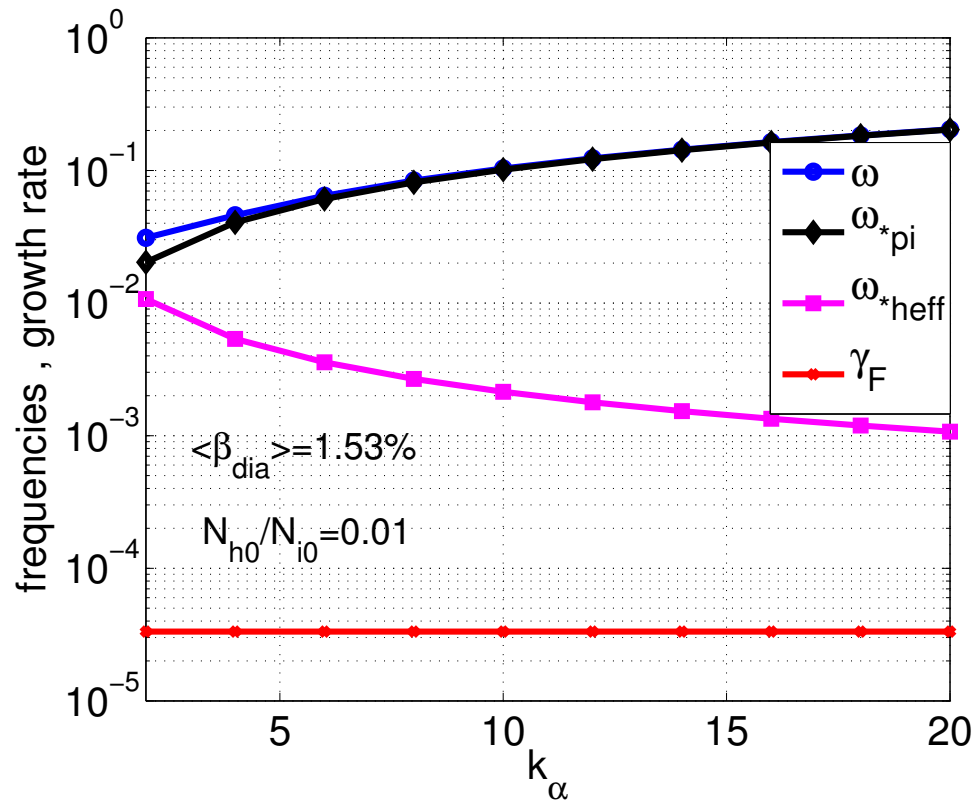
- Thermal ion diamagnetic drift

- Effective hot particle diamagnetic drift



Mode and Diamagnetic Drift Frequencies

- Frequencies at $\langle \beta_{dia} \rangle = 1.53\%$ versus k_α and $\langle \beta_{dia} \rangle = 4.5\%$ versus N_{h0}/N_{i0}



- Note that $|\omega_{*pi} + \omega_{*heff}|/2 \gg \gamma_F$

- Major assumption $\omega \ll \omega_{dh}$.

- Definition of ω_{dh}

- ▷ single particle drift: $\hat{\omega}_{dj} = -(\omega_{\kappa} v_{\parallel}^2 + \omega_B v_{\perp}^2/2)/\Omega_j$

where $\omega_{\kappa} \equiv \mathbf{B} \times \mathbf{k}_{\perp} \cdot \boldsymbol{\kappa}/B$, $\omega_B \equiv \mathbf{B} \times \mathbf{k}_{\perp} \cdot \nabla B/B^2$,
 $\Omega_j \rightarrow$ cyclotron frequency for species j .

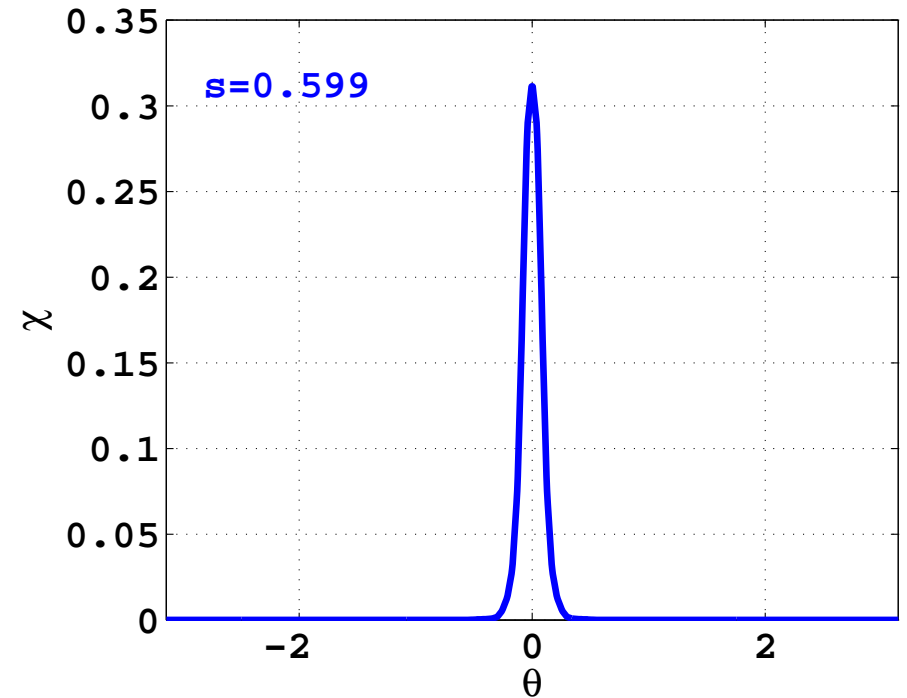
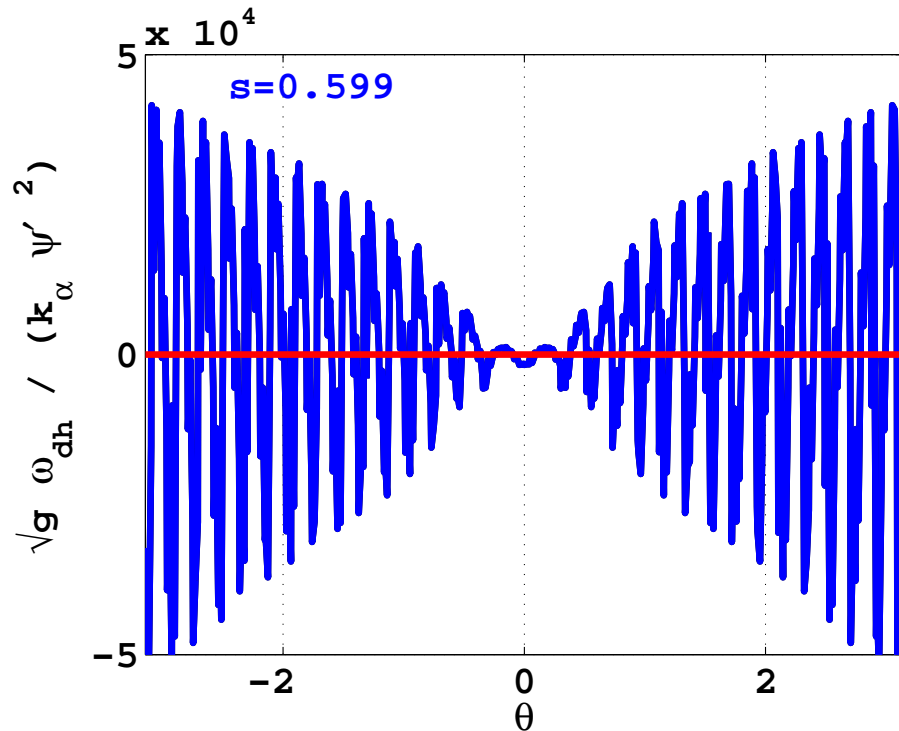
- ▷ velocity space averaged hot particle drifts

$$\omega_{dh} = \frac{\int d^3v F_{0h} \hat{\omega}_{dh}}{\int d^3v F_{0h}}$$

- ▷ Mode-width weighted hot particle drifts

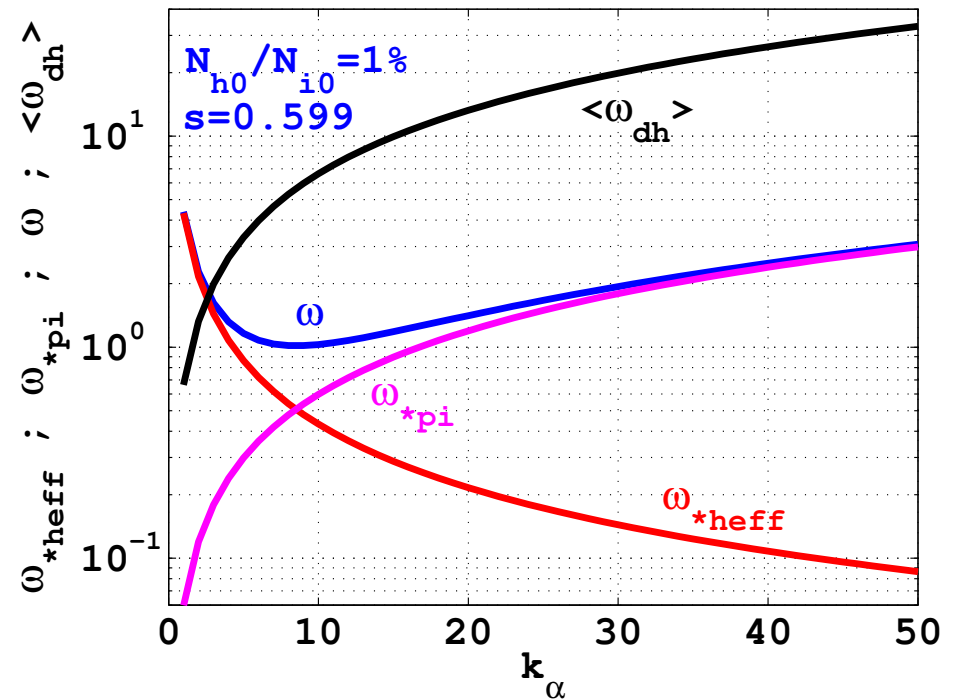
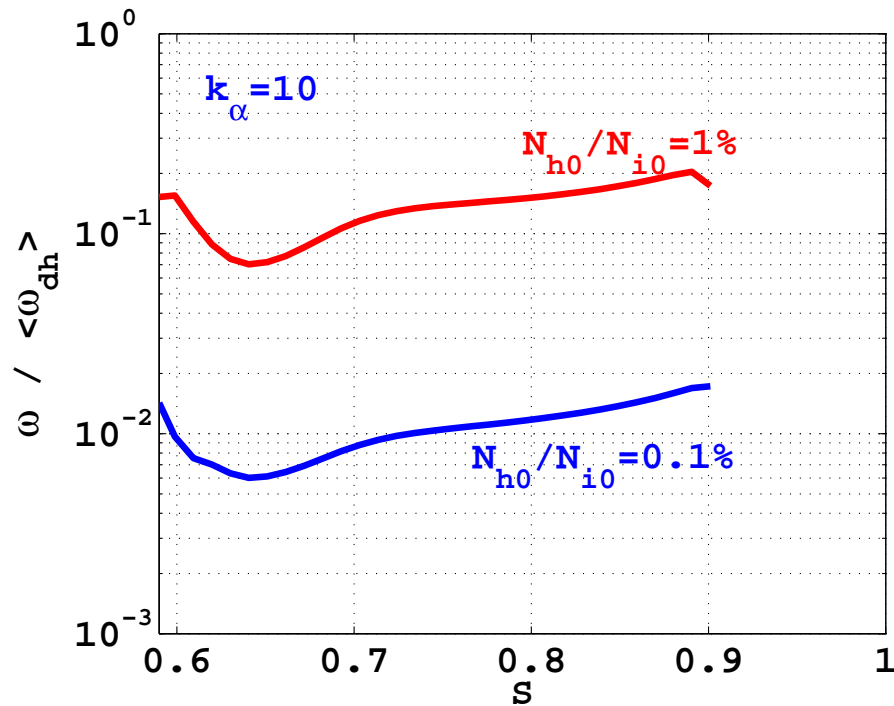
$$\langle \omega_{dh} \rangle = \frac{\int_{-\infty}^{\infty} d\theta (\sqrt{g}/\psi') \omega_{dh} |\chi|^2}{\int_{-\infty}^{\infty} d\theta (\sqrt{g}/\psi') |\chi|^2}$$

- Normalised v -space averaged hot particle drift
- Ballooning eigenfunction



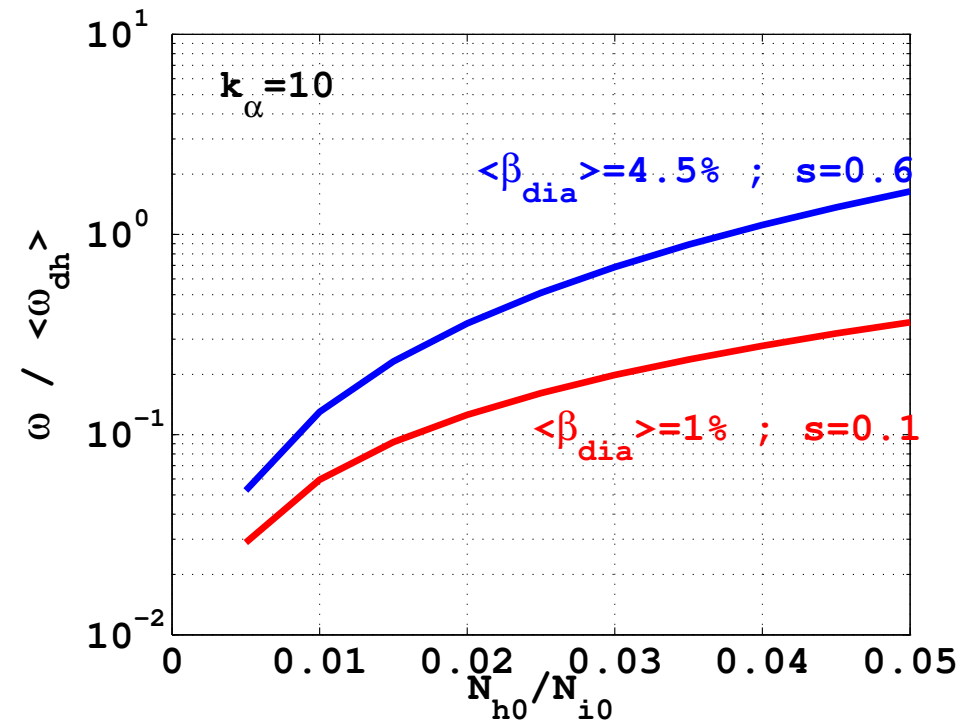
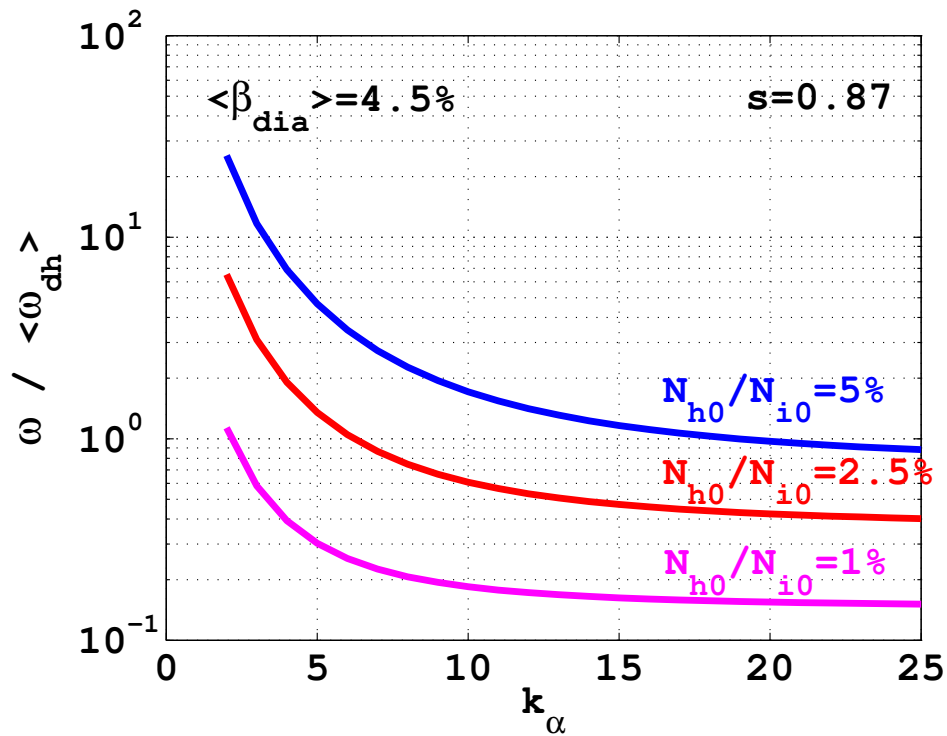
- Contend that hot particle drift is most relevant where mode localises

- Mode to hot particle drift frequency ratio
- Frequency dependencies on k_α



- ω_{*heff} only important at small k_α where theory breaks down

- Mode to hot particle drift frequency ratio as functions of k_α and N_{h0}/N_{i0} .



- Ballooning stability can impose very strict operating constraints in current-free stellarators.
- We have applied a ballooning mode theory based on large hot particle drifts and finite diamagnetic drift corrections to a model LHD heliotron with $\langle \beta_{dia} \rangle$ up to 4.8% (a value achieved experimentally).
- The fluid limit (with reduced hot particle pressure gradient drive and absence of diamagnetic drifts) predicts a ballooning unstable band that moves from the plasma core at low $\langle \beta_{dia} \rangle$ to the plasma boundary at $\langle \beta_{dia} \rangle \simeq 5\%$ encompassing roughly 1/3 of the plasma volume.
- Including diamagnetic drifts, this theory predicts that the LHD device is stable to ballooning modes as $|\omega_{*pi} + \omega_{*heff}|/2 > \gamma_F$ for $0 \leq \langle \beta_{dia} \rangle \leq 4.8\%$.

- We have verified that the ballooning mode frequency is much smaller than the mode-width averaged hot particle (curvature and ∇B) drifts for $N_{h0}/N_{i0} \leq 2\%$ (except for small k_α). This confirms that the expansion in ω/ω_{dh} was justified.
- We find that the effective hot particle diamagnetic drift has a weak impact on stability properties compared with the thermal ion diamagnetic drift. This is consistent with the fact that if the hot particle drifts (curvature and/or ∇B) are too fast to contribute significantly to the instability drive, they must also have a feeble impact on stability.
- The results obtained suggest that drift-magnetohydrodynamics may constitute a more appropriate model for current-free stellarator/heliotron stability than ideal MHD or other enhanced (anisotropic) single fluid approaches.

- ▶ Total parallel pressure

$$p_{\parallel}(s, B) = p(s) + \mathcal{N}(s)T_{\parallel}(s)H(s, B)$$

- ▶ FOR $B > B_C$:

$$H(s, B) = \frac{(B/B_C)}{\left[1 - \frac{T_{\perp}}{T_{\parallel}} \left(1 - \frac{B}{B_C}\right)\right]}$$

- ▶ FOR $B < B_C$:

$$H(s, B) = \frac{B}{B_C} \frac{\left[1 + \frac{T_{\perp}}{T_{\parallel}} \left(1 - \frac{B}{B_C}\right) - 2 \left(\frac{T_{\perp}}{T_{\parallel}}\right)^{5/2} \left(1 - \frac{B}{B_C}\right)^{5/2}\right]}{\left[1 - \left(\frac{T_{\perp}}{T_{\parallel}}\right)^2 \left(1 - \frac{B}{B_C}\right)^2\right]}$$

• At low $\langle \beta_{dia} \rangle$

• At high $\langle \beta_{dia} \rangle$

